Design of Port Plate in Gerotor Pump for Reduction of Pressure Pulsation

Sang-Yeol Kim, Yun-Joo Nam
Department Mechanical and Intelligent Systems Engineering, Pusan National Universiy, 30 Jangjeon-dong, Geumjeong-gu, Busan 609-735, Korea
Myeong-Kwan Park*
Research Institute of of Mechanical Technoloty, School of Mechanical Engineering, Pusan National University, 30 Jangjeon-dong, Geumjeong-gu, Busan 609-735, Korea

The pressure pulsation due to the gear geometry of the gerotor (generalized rotor) pump mainly occurs in an instant that the chamber of the gerotor enters the delivery port and leaves the suction one. Such a pressure pulsation may result in undesirable vibration and noise of pump components as well as cavitation in hydraulic system. Therefore, it is very important to examine the pressure characteristic of the gerotor pump at its design and analysis stages. In this paper, in order to reduce the pressure pulsation in the gerotor pump, the port plate with the relief grooves is designed by referring to as notch of vane pump and relief groove of piston pump. A series of the theoretical analyses on the pressure pulsation is performed in consideration of various design parameters of the port plate, including the installation positions of the port inlet/outlet and the groove width, and the operating conditions such as rotational velocity and delivery pressure.

Key Words : Gerotor Pump, Relief Groove, Port Plate, Pressure Pulsation

1. Introduction

A gerotor pump, so called generalized rotor pump, is advantageous in miniaturizing the applied systems due to its simpler structure and higher delivery flow rate-to-volume than other hydraulic pumps such as vane and piston counterparts (Mancó et al., 1998). Moreover, its high mechanical and volumetric efficiencies resulting from small relative rotation velocity between inner and outer rotors as well as its reliability in long term operation environment bring out the applications of the gerotor pump to more and more industrial fields, such as lubrication oil pump for automobile engine and hydraulic source for power transmission devices.

However, the gear geometry of the gerotor leads pressure pulsations in an instant that the chamber generated by conjugation of inner and outer rotors enters the delivery port and leaves the suction one. These pressure pulsations may result in undesirable vibration and noise of pump components as well as cavitation in hydraulic system. Therefore, it is very important to examine the pressure characteristic of the gerotor pump at its design and analysis stages.

Most of the previous researches on the gerotor pump have been concentrated on its gear formation and design (Beard et al., 1989 ; Colbourne, 1974 ; Demenego et al., 2002 ; Litvin and Feng, 1996 ; Manfred and Adam, 2001 ; Mimmi and Pennacchi, 1997 ; Saegusa et al., 1984). Also, some

* Corresponding Author,
E-mail : mkpark1@pusan.ac.kr
TEL : +82-51-510-2464; **FAX** : +82-51-514-0685
Research Institute of of Mechanical Technoloty, School of Mechanical Engineering, Pusan National University, 30 Jangjeon-dong, Geumjeong-gu, Busan 609-735, Korea. (Manuscript **Received** February 2, 2006; **Revised** July 10, 2006)

researchers have investigated the wear and mechanical stress occurred at the contact points between inner and outer rotors (Beard, 1992; Gamez-Montero and Codina, 2000; Kim et al., 2000). However, these results did not considered the geometry of the inlet and outlet installed on the port plate, through which the operating fluid comes in and goes out, and therefore, it is difficult to effectively evaluate the effects of pressure pulsations on the dynamic characteristics of the gerotor pump.

As a consequence, the aim of this paper is to design of the port place in the gerotor pump and to investigate the effects of its design parameter on pressure pulsations. First of all, the relief grooves are installed at the inlet of the delivery port and the outlet of the suction one, referring to as the notch of vain pumps (Kim et al., 1998a and 1998b) and the relief groove of piston pumps (Harris et al., 1994; Harrison and Edge, 2000; Manring, 2000 and 2003). Then, in order to reduce undesired pressure pulsations, the design parameters of the relief groove are optimized through a series of the theoretical analyses performed in consideration of the installation positions of the port inlet/outlet, the groove width and the operating conditions such as rotational velocity and delivery pressure. The results presented in this paper can be effectively used as a basic material for the development of the gerotor pump with higher performance and reliability as well as for the expansion of its applicability.

2. Gerotor Geometry and Operationg Principle

As can be seen in Fig. 1, the gerotor pump consists of an inner rotor in sliding contact with an outer rotor and the port plate including the suction and delivery ports. It is a major characteristic of the gerotor pump that the inner rotor has one less lobe than the outer counterpart. Since the inner rotor rotates continuously contacting with the outer rotor, a variety of the chambers are generated by conjugating two rotors so that the operating fluid can be transferred from the suction port to the delivery port.

The outer rotor has N lobes with its radius of S equally distributed on a circle with its radius S and its center at O_e. The center of the inner rotor is positioned at O_i departed with the eccentricity of e from O_e. The inner and outer pitch circles, which are respectively centered at O_i and O_e, always rotate in identical direction with relative velocity of $N/(N-1)$.

The area of the j-th chamber, $A_j(\alpha)$ for $j=1,2,\cdots,N$, obtained when the outer rotor counter-clockwise rotates equally to the rotation angle α with respect to the reference position $\alpha=0$ [deg] presented in Fig. 2, can be given by

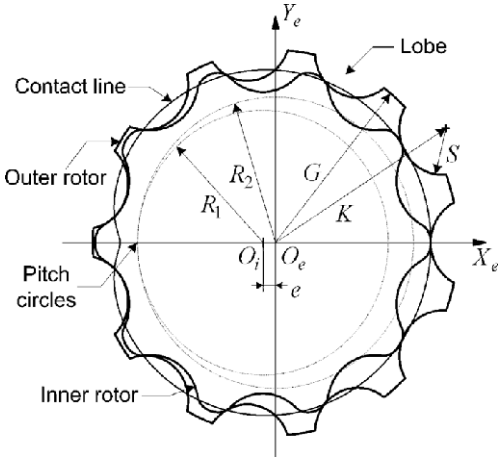

Fig. 1 Schematic configuration of the gerotor

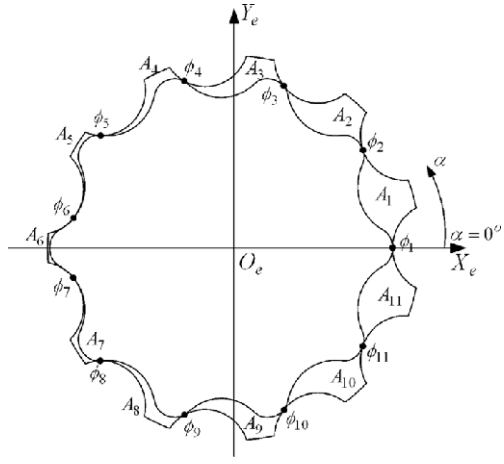

Fig. 2 Reference position and numbering of the chambers and contact points

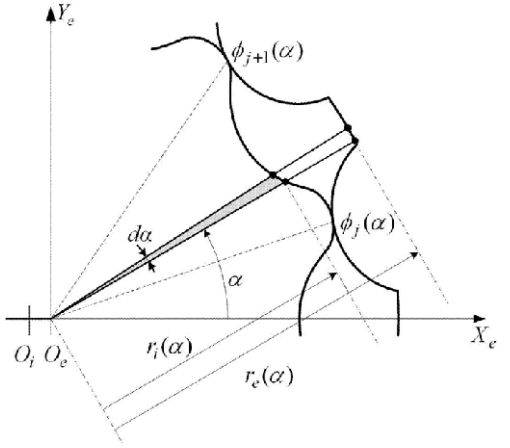

Fig. 3 Integral calculation for the chamber area

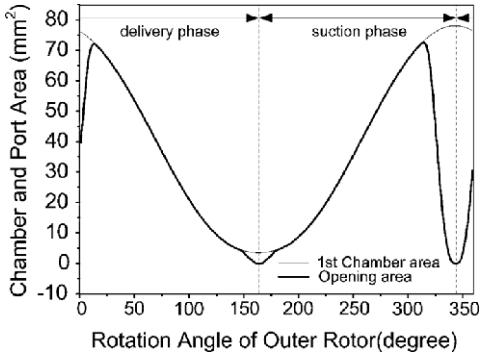

Fig. 4 The first chamber area with respect to the rotation angle and the corresponding opening areas

$$A_j(\alpha)=\frac{1}{2}\int_{\phi_j(\alpha)}^{\phi_k(\alpha)}[r_e^2(\alpha)-r_i^2(\alpha)]\,d\alpha, \quad \begin{cases} k=j+1 & (j\neq N) \\ k=1 & (j=N) \end{cases} \tag{1}$$

where $r_i(\alpha)$ and $r_e(\alpha)$ represent, respectively, the distances from O_e to the inner and outer rotor obtained at α, as can be seen to in Fig. 3. It is noted that they are given as the function of the corresponding gear formation. Fig. 4 shows the first chamber area $A_1(\alpha)$ with respect to the rotation angle, obtained by using the gerotor designed under the specification given in Table 1. This gerotor is used as an example for the design of the port plate, and the derivation procedure for its gear formation can be found from various references presented in this paper (Beard et al., 1989; Colbourne, 1974; Demenego et al., 2002; Litvin and Feng, 1996; Manfred and Adam, 2001; Mimmi and Pennacchi, 199; Saegusa et al., 1984). While the chamber area is increased, the pressure within it lowers below the atmosphere so that the operating fluid comes in from the tank. On the other hand, while chamber area is decreased, the pressure within it rises above the atmosphere so that the operating fluid goes out to the tank.

Table 1 Specifications of the gerotor

Design parameter	Value
Number of lobes in outer rotor : N	11
Eccentricity : e	2.2 [mm]
Radius of lobes in outer rotor : S	7.5 [mm]
External radius of outer rotor : G	32.0 [mm]
Distance between lobe center and origin : K	34.4 [mm]
Thickness of the gerotor	10.0 [mm]
Radius of outer pitch circle : $R_2=N\cdot e$	24.2 [mm]
Radius of inner pitch circle : $R_1=(N-1)\cdot e$	22.0 [mm]

3. Theoretical Analysis on Pressure Pulsation

In this paper, the theoretical approaches to the pressure pulsation of the gerotor pump are achieved under the following two assumptions: the operating fluid is incompressible, and the flow leakages are negligible. The former is valid since the isentropic bulk modulus of the operating fluid is generally given by 1.62×10^9 [Pa], and the latter is conceivable in order to avoid the complexity of the analysis.

While the gerotor rotates, the operating fluid comes in and goes out of the chamber through the opening areas between the chamber and the ports. Therefore, the chamber and the opening areas can be, respectively, considered by the control volume and the variable orifice, and then, the delivery and suction flow rates, Q_d and Q_s, through the j-th opening area are described as follows

$$Q_{jd,s}=\mathrm{sgn}(P_{d,s}-P_j)\,C_q A_{d,s}\sqrt{\frac{2}{\rho}|P_{p,s}-P_j|}, \quad \text{for } j=1,2,\cdots,N \tag{2}$$

where P_d is the delivery pressure, P_s is the suction pressure, ρ is the density of the operating fluid given by 875 [kg/m^3], P_j is the pressure of

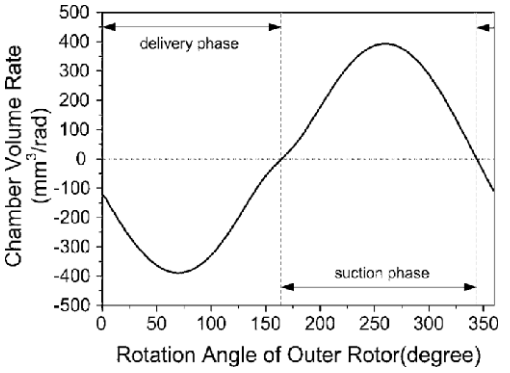

Fig. 5 The first chamber volume rate with respect to the rotation angle

the j-th chamber, and C_q is the flow coefficient given by 0.68, respectively. Also, A_d and A_s represent the opening areas of the delivery and suction ports.

Moreover, the delivery and suction flow rates related to the volume variation of the j-th chamber with respect to time, V_j, can be obtained as

$$Q_{jd,s}=\frac{dV_j}{dt}=\frac{dV_j}{d\alpha}\omega=\frac{d(A_j\cdot H)}{d\alpha}\omega, \quad \text{for } j=1,2,\cdots,N \tag{3}$$

where H is the thickness of the gerotor and ω is the rotation velocity of the outer rotor. The volume rate with respect to the rotation angle, dV_1/d_α, is represented in Fig. 5.

Then, substituting Eq. (2) into Eq. (3), the pressure within the j-th chamber can be given by

$$P_j=P_{d,s}-\mathrm{sgn}\left(\frac{dV_j}{dt}\right)\cdot\left(\frac{dV_j/d\alpha}{C_q\cdot A_{d,s}}\omega\right)^2\frac{\rho}{2}, \quad \text{for } j=1,2,\cdots,N \tag{4}$$

in which, it is noted that the second term in the right-hand side describes the pressure pulsations. Therefore, we can clearly see that the pressure pulsation within the chamber is related to the geometric variables of the gerotor and port plate, $dV_j/d\alpha$ and $A_{d,s}$ as well as the operating conditions, $P_{d,s}$ and $A_{d,s}$.

4. Design of Relief Groove on Port Plate

Considering the bulk modulus of the operating fluid requiring the pressure variation of approximately 17000 [kPa] for the volume variation ratio of 1 [%], the distance between the inlet of the delivery port and the outlet of the suction one should be equal to the overall length of one chamber. If the distance becomes smaller than the chamber length (so called overlapped condition), the delivery and suction ports are passed through each other so that the volumetric efficiency of the gerotor pump is degraded due to the delivery flow loss from the delivery port to the suction one. On the other hand, if the distance becomes longer (so called underlapped condition), the pressure of the chamber can be seriously increased due to the bulk modulus of the operating fluid so that the gerotor pump can be locked or be destroyed.

As can be seen in Fig. 6, if both pointed end of the chamber are engaged with the edge of each port where the chamber volume become to be maximized (at 343.64 [degree]), then the chamber area can be obtained from the maximally extreme value in Fig. 4 and the corresponding chamber pressure is shown in Fig. 7. Here, we can see clearly that the pressure within the chamber is severely varied, since the opening area $A_{d,s}(\alpha)$ is shrunken in the instant that the chamber comes into the delivery port and goes out of the suction port, as can be seen in Fig. 4. The pressure drop occurring while the chamber passes through the suction port (increasing volume phase) can cause the cavitation phenomenon of the pump, and the pressure rise while the chamber contacts with the delivery port (decreasing volume phase) is sufficient for the breakdown of the pump. In addition, these pressure pulsations are major source of undesired vibration and noise of the operating fluid and the pumping system. Therefore, it is very important to reduce these pressure pulsations in order to guarantee the stable performance and reliable operation of the pump. For these reasons, the notch or relief groove is being installed on the port plates in vane and piston pumps in order to gradually control the opening area and to smoothly derive the pressure variations.

In this section, the port plate in the gerotor pump is designed by referring to such a nature of the relief groove. Considering that both pointed

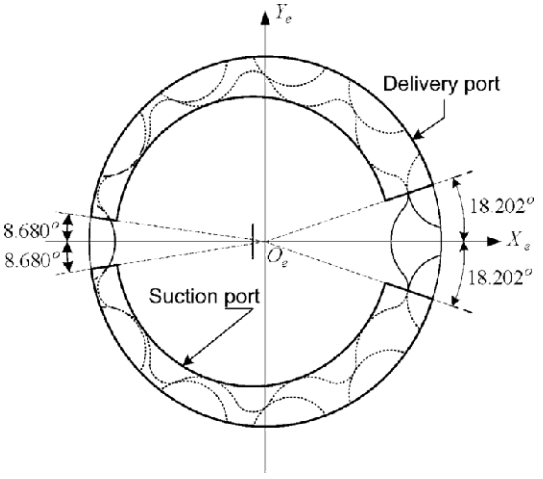

Fig. 6 Schematic configuration of the suction and delivery ports

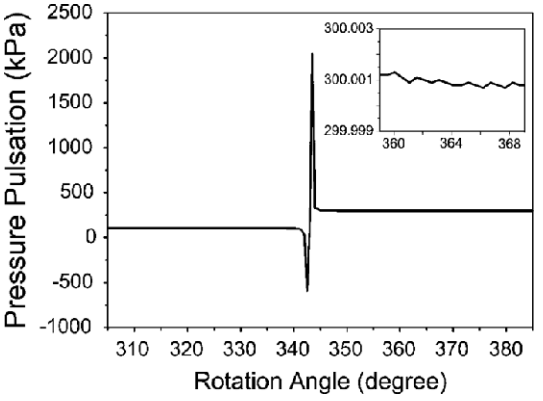

Fig. 7 Pressure pulsation in the first chamber without the relief groove

points of the chamber inevitably generated due to the geometry of the gerotor are impossible to be modified, the grooves for the gerotor can be designed, as described in the following sections:

4.1 Suction port

Figure 8 shows the design parameters for the suction port. The suction groove depicted by $A'B'C'D'$ is installed in order to extend the partial outlet of the suction port so that the section $A'-D'$ of the groove is positioned on the edge of the lobe in the instant that the chamber leaves the port. Therefore, the opening area between the chamber and the port can be effectively increased

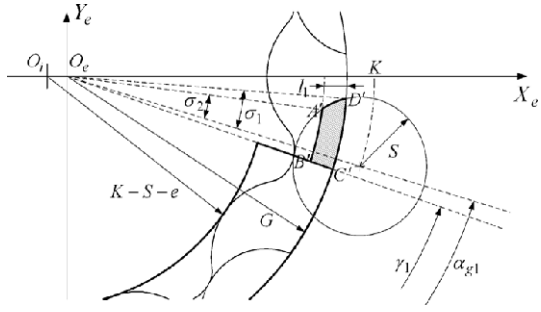

Fig. 8 Design parameters for the suction port and groove

while the chamber area is increased, especially, in the instant that the chamber leaves the suction port.

The primary design parameters include the width of the suction groove width l_1 and the port reference angle α_{g1} determining the port installation position. And, σ_1, σ_2, and γ_1 are the dependent variables given as the function of the design parameters for the gerotor and the suction port l_1 and α_{g1}, which are expressed by

$$\sigma_1=\arctan\left(\frac{y_o}{x_o}\right),\ \begin{cases}x_o=(K^2+G^2-S^2)/(2K)\\ y_o=\sqrt{G^2-x_o^2}\end{cases} \tag{5}$$

$$\sigma_2=\arctan\left(\frac{y_1}{x_1}\right),\ \begin{cases}x_1=\{K^2+(G^2-l_1)^2-S^2\}/(2K)\\ y_1=\sqrt{(G-l_1)^2-x_1^2}\end{cases} \tag{6}$$

$$\gamma_1=\arctan\left(\frac{y_{g1}}{x_{g1}}\right),$$
$$\begin{cases}x_{g1}=K\cos(\alpha_{g1})-S\{K\cos(\alpha_{g1})+R_1\}/T_1\\ y_{g1}=K\sin(\alpha_{g1})-SK\sin(\alpha_{g1})/T_1\\ T_1=\sqrt{R_1^2+K^2+2R_1K\cos(\alpha_{g1})}\end{cases} \tag{7}$$

where $R_1=N\cdot e$ is the radius of the outer pitch circle, K is the distance between the center of the outer rotor O_e and the centers of the lobes, G is the external radius of the outer rotor, and is the lobe radius of the outer rotor, as shown in Fig. 1. Then, the opening area A_{g1} of the suction groove with respect to the rotation angle of the outer rotor can be derived as

$$A_{g1}=A'_{op}-A'_{cl} \tag{8}$$

where A'_{op} is the opening area in the open phase where the chamber come in the suction groove as can be seen in Fig. 10(c), and A'_{cl} in the closed phase where the chamber goes out of the suction groove as can be seen in Fig. 10(d).

$$A'_{op}=\begin{cases}0 & (\alpha'\le\sigma_2-\alpha_{g1}+\gamma_1)\\ \dfrac{1}{2}\left\{\dfrac{\alpha'-(\sigma_2-\alpha_{g1}+\gamma_1)}{\sigma_1-\sigma_2}\right\}^2(G-l_1)\cdot l_1(\sigma_1-\sigma_2) & (\sigma_2-\alpha_{g1}+\gamma_1\le\alpha'<\sigma_1-\alpha_{g1}+\gamma_1)\\ \dfrac{1}{2}(G-l_1)\cdot l_1(\sigma_1-\sigma_2)+\dfrac{1}{2}(2Gl_1-l_1^2)\{\alpha'-(\sigma_2-\alpha_{g1}+\gamma_1)\} & (\sigma_1-\alpha_{g1}+\gamma_1\le\alpha'<2\sigma_2)\\ \dfrac{1}{2}(G-1_l)\cdot l_1(\sigma_1-\sigma_2)+\dfrac{1}{2}(2Gl_1-l_1^2)\{2\sigma_2-(\sigma_1-\alpha_{g1}+\gamma_1)\}+\left\{1-\left(1-\dfrac{\alpha'-2\sigma_2}{2(\sigma_1-\sigma_2)}\right)\right\}^2Gl_1(\sigma_1-\sigma_2) & (2\sigma_2\le\alpha'<2\sigma_1)\\ \dfrac{1}{2}Gl_1(\sigma_1+\sigma_2+2\alpha_{g1}-2\gamma_1)-\dfrac{1}{2}l_1^2(\sigma_2+\sigma_{g1}+\gamma_1) & (2\sigma_1\le\alpha'<2\pi/N)\end{cases}$$

$$A'_{op}=\begin{cases}0 & (\alpha'<2\pi/N-\sigma_1-\alpha_{g1}+\gamma_1)\\ \dfrac{1}{2}\left\{\dfrac{\alpha'-(2\pi/N-\sigma_1-\alpha_{g1}+\gamma_1)}{\sigma_1-\sigma_2}\right\}^2Gl_1(\sigma_1-\sigma_2) & (2\pi/N-\sigma_1-\alpha_{g1}+\gamma_1\le\alpha<2\pi/N-\sigma_2-\alpha_{g1}+\gamma_1)\\ \dfrac{1}{2}Gl_1(\sigma_1-\sigma_2)+\dfrac{1}{2}(2Gl_1-l_1^2)\{\alpha'-(2\pi/N-\sigma_1-\alpha_{g1}+\gamma_1)\} & (2\pi/N-\sigma_1-\alpha_{g1}+\gamma_1\le\alpha'\le2\pi/N)\end{cases}$$

in which $\alpha'=\alpha-\alpha_{g1}$.

4.2 Delivery port

Figure 9 shows the design parameters for the delivery port. Similar to the suction ports, the delivery groove depicted to $A''B''C''D''$ is installed in order to extend the partial outlet of the delivery port so that the section $B''-C''$ is positioned on the edge of the lobe at the instant that the chamber comes into the port. The primary design parameters are the width of the delivery groove width l_2 and the port reference angle $\alpha_{g2}=\alpha_{g1}+2\pi/N$ determining the port installation position. The additionally introduced variables σ_3 and γ_2 are given by

$$\sigma_3=\arctan\left(\frac{y_2}{x_2}\right),\quad \begin{cases}x_2=\{K^2+(G-l_2)^2-S^2\}/(2K)\\ y_2=\sqrt{(G-l_2)^2-x_2^2}\end{cases}\tag{9}$$

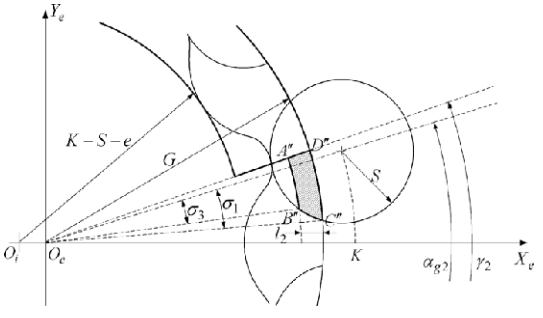

Fig. 9 Design parameters for the delivery port and groove

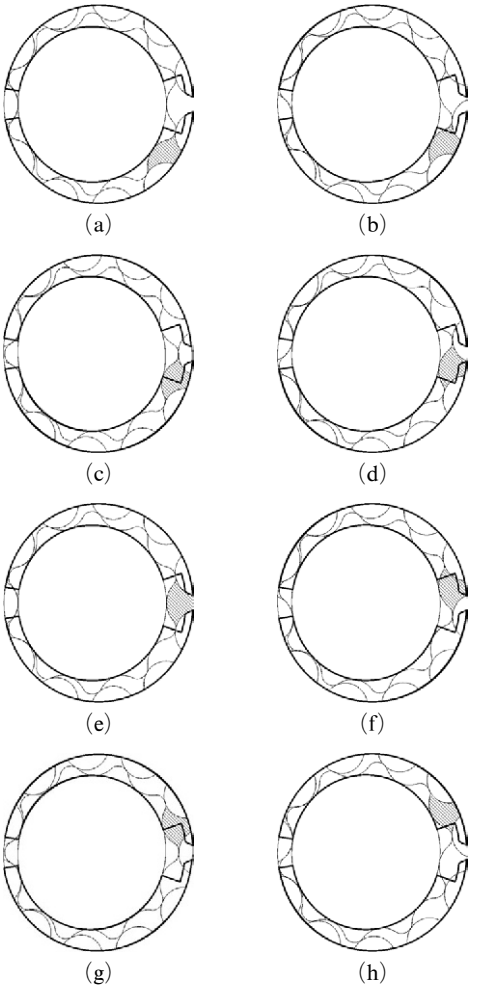

Fig. 10 Panoramic phases of the chamber and opening areas

$$\gamma_2=\arctan\left(\frac{y_{g2}}{x_{g2}}\right),$$

$$\begin{cases} x_{g2}=K\cos(\alpha_{g2})-S\{K\cos(\alpha_{g2})+R_1\}/T_2 \\ y_{g1}=K\sin(\alpha_{g2})-SK\sin(\alpha_{g2})/T_2 \\ T_2=\sqrt{R_1^2+K^2+2R_1K\cos(\alpha_{g2})} \end{cases} \quad (10)$$

Then, the opening area A_{g2} of the delivery port with respect to the rotation angle of the outer rotor can be derived as

$$A_{g2}=A''_{op}-A''_{cl} \quad (11)$$

where A''_{op} is the opening area in the open phase where the chamber come in the delivery groove ac can be seen in Fig. 10(f), and A''_{cl} in the closed phase where the chamber goes out of the delivery groove as can be see in Fig. 10(g)

$$A''_{op}=\begin{cases} \frac{1}{2}(2Gl_2-l_2^2)\cdot\alpha'' & (\alpha''<\gamma_2-\alpha_{g2}+\sigma_3) \\ \frac{1}{2}(2Gl_2-l_2^2)\cdot\alpha''-\frac{1}{2}\left\{\frac{\alpha''-(\gamma_2-\alpha_{g2}+\sigma_3)}{\sigma_1-\sigma_3}\right\}^2(G-l_2)\cdot l_2(\sigma_1-\sigma_3) & (\gamma_2-\alpha_{g2}+\sigma_3\le\alpha''<\gamma_2-\alpha_{g2}+\sigma_1) \\ \frac{1}{2}(2Gl_2-l_2^2)(\gamma_2-\alpha_{g2}+\sigma_1)-\frac{1}{2}(G-l_2)\cdot l_2(\sigma_1-\sigma_3) & (\gamma_2-\alpha_{g2}+\sigma_1\le\alpha''<2\pi/N) \end{cases}$$

$$A''_{cl}=\begin{cases} 0 & (\alpha''<2\pi/N-2\sigma_1) \\ \left\{\frac{\alpha''-2\pi/N+2\sigma_1}{2(\sigma_1-\sigma_3)}\right\}^2 Gl_2(\sigma_1-\sigma_3) & (2\pi/N-2\sigma_1\le\alpha''<2\pi/N-2\sigma_3) \\ Gl_2(\sigma_1-\sigma_3)+\frac{1}{2}(2Gl_2-l_2^2)\{\alpha''-(2\pi/N-2\sigma_3)\} & (2\pi/N-2\sigma_3\le\alpha''<2\pi/N+\gamma_2-\alpha_{g2}-\sigma_1) \\ Gl_2(\alpha_1-\sigma_3)+\frac{1}{2}(2Gl_2-l_2^2)(\gamma_2-\alpha_{g2}-\sigma_1+2\sigma_3)+\frac{1}{2}\left\{1-\left(1-\frac{\alpha''-(2\pi/N+\gamma_2-\alpha_{g2}-\sigma_1)}{\sigma_1-\sigma_3}\right)\right\}^2(G-l_2)\,l_2(\sigma_1-\sigma_3) & \\ \qquad (2\pi/N+\gamma_2-\alpha_{g2}-\sigma_1\le\alpha''<2\pi/N+\gamma_2-\alpha_{g2}-\sigma_3) & \\ \frac{1}{2}(2Gl_2-l_2^2)(\gamma_2-\alpha_{g2}+\sigma_1)-\frac{1}{2}(G-l_2)\,l_2(\sigma_1-\sigma_3) & (2\pi/N+\gamma_2-\alpha_{g2}-\sigma_3\le\alpha''<2\pi/N) \end{cases}$$

in which $\alpha''=\alpha+2\pi/N-\alpha_{g1}$

5. Analsys Results and Discussion

In this section, the effects of the port design parameters including the width of the relief grooves l_i and the port reference angles α_{gi} for $i=1,2$ as well as the operating conditions, $P_{d,s}$ and A_{ds}, on the pressure pulsation of the gerotor pump are investigated theoretically.

5.1 Position of the suction port and width of the relief groove

Figure 11 shows the pressure pulsations with respect to the suction groove width l_1 and the port reference position α_{g1}, from which we can see that the closer the port reference position is to the position for the chamber volume to be maximized (343.64 [degree]), the more decreased the pressure undershoot is for a specified groove width. This means that the pressure drop can be significantly decreased in the case that the volume rate with respect to the rotation angle become close to zero. Therefore, we can conclude that the effective orifice term in Eq. (4) is closely connected with the volume rate of the chamber. Moreover, Fig. 11 shows that the pressure undershoots are shapely decreased with the increase of the groove width. Especially, we can see that the pressure drop at about 343.64 [degree] becomes approximately −600 [kPa] without the groove, while the pressure drop is effectively decreased even with small groove width. Although the small groove width is enough to decrease the cavitation in the pump, the groove width as large as possible is preferred in order to attenuate the pressure pulsation generating undesired vibration and noise. Fig. 13 represents the groove width maximally obtainable at the given rotation angle of the outer rotor, which is dependent on the geometry of the applied gerotor.

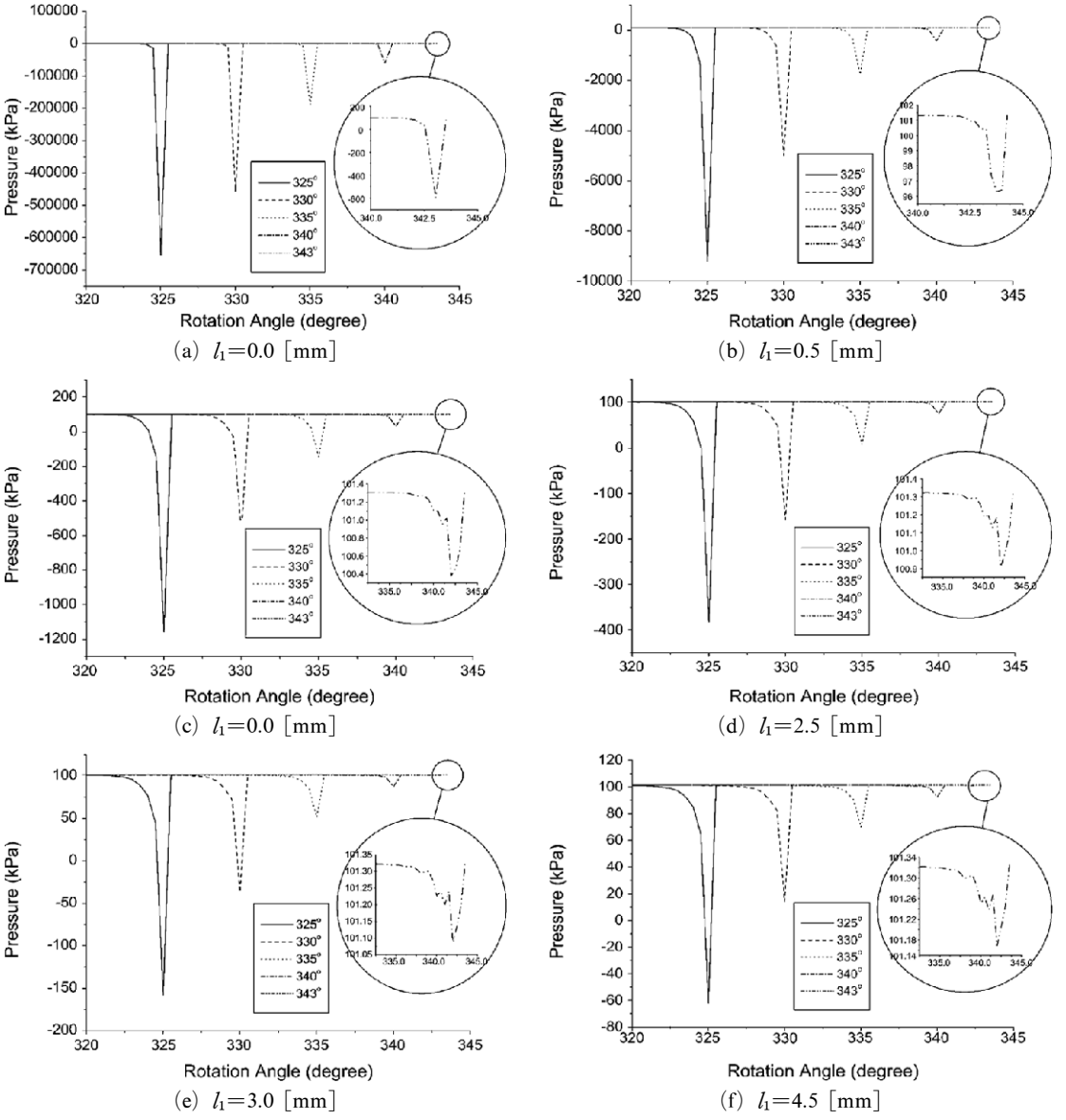

(a) l_1=0.0 [mm] (b) l_1=0.5 [mm]

(c) l_1=0.0 [mm] (d) l_1=2.5 [mm]

(e) l_1=3.0 [mm] (f) l_1=4.5 [mm]

Fig. 11 Pressure pulsation with respect to the groove width and the reference position for the suction port

5.2 Position of the delivery port and width of the relief groove

Figure 12 shows the pressure pulsation with respect to the delivery groove width l_2 and the port reference position α_{g2}. In this case, the pressure pulsation analysis should be performed only in the increasing chamber volume phase. If the chamber is connected with the delivery port in the decreasing chamber volume phase, then the operating fluid, which is flowed in the chamber through the suction port until the chamber volume is to be maximized, is backward flowed to the suction port while the volume decreases. Since this causes the delivery flow loss of the gerotor pump, such a situation should be excluded at the design stage of the port plate. As can be seen in Fig. 12, the pressure pulsation is significantly decreased at which the volume rate with respect to the rotation angle is near to zero, that is, at the position for the chamber volume to be maximized.

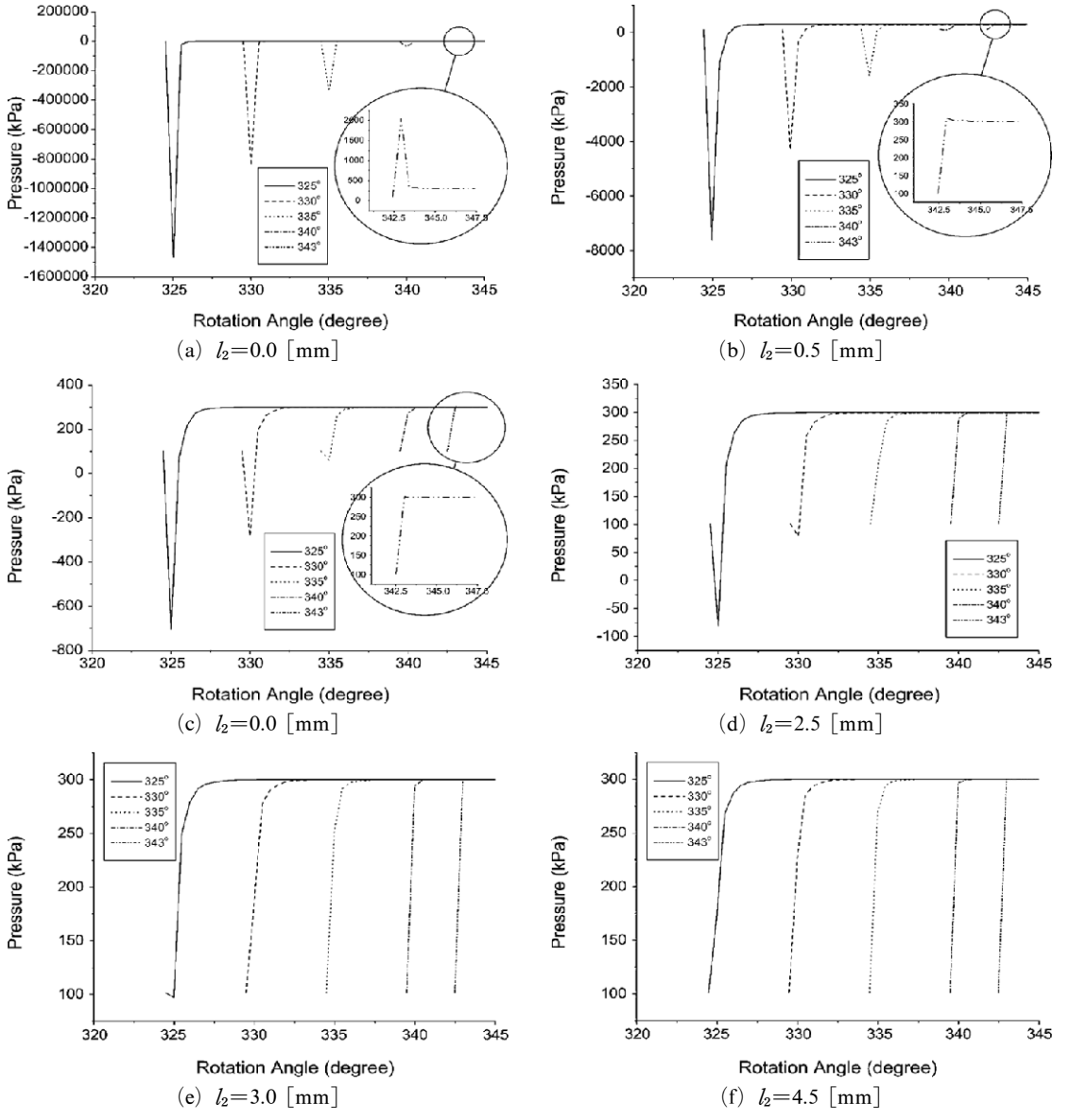

(a) l_2=0.0 [mm] (b) l_2=0.5 [mm]

(c) l_2=0.0 [mm] (d) l_2=2.5 [mm]

(e) l_2=3.0 [mm] (f) l_2=4.5 [mm]

Fig. 12 Pressure pulsation with respect to the groove width and the reference position for the delivery port

In addition, we can see that the pressure pulsations are remarkably decreased and the region where the pressure is smoothly increased without undershoot of the pressure is extended, when the groove width is increased. Especially, in the case that the groove width is larger than 3.5 [mm], the farther the port reference position is from 343.64 [degree], the more smoothly the chamber pressure is increased to the delivery pressure in 300 [kPa]. This is because the operating fluid is discharged from the delivery port while the chamber volume is increased but the volume rate is decreased, which can be verified through the comparison of Figs. 4 and 5.

5.3 Delivery pressure

Figure 14 shows the pressure pulsation according to the variation of the delivery pressure, investigated under the following conditions: the rotation velocity is 1000 [rpm], the width suction

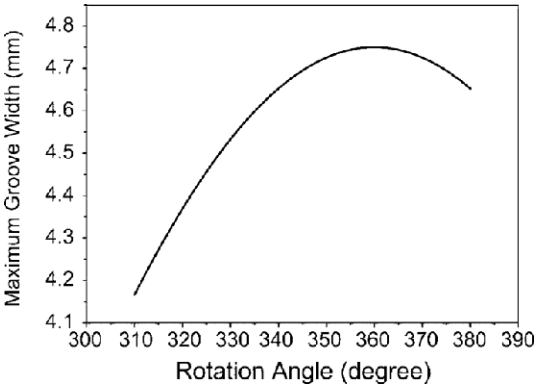

Fig. 13 Maximally allowable groove width with respect to the rotation angle

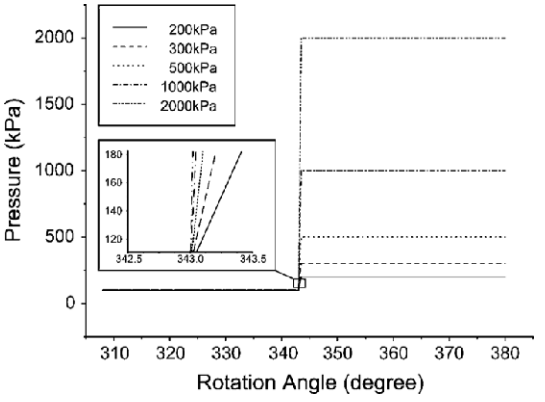

Fig. 14 Pressure pulsation with respect to the delivery pressures

and delivery grooves is 4.5 [mm], and the port reference position of the suction port is 343 [degree]. We can clearly see that despite of the variation of the delivery pressures in the range of 200～2000 [kPa], the resultant chamber pressures is increased to the given delivery pressure without any pulsation. This is because the effective orifice term in Eq. (4) is independent of the delivery pressure. Therefore, we can conclude that the proposed port plate dose not bring about any pressure pulsation due to the variation of the delivery pressure.

5.4 Rotational velocity

Figure 15 shows the pressure pulsation with respect to the rotation velocity of the gerotor, performed with the delivery pressure of 300 [kPa],

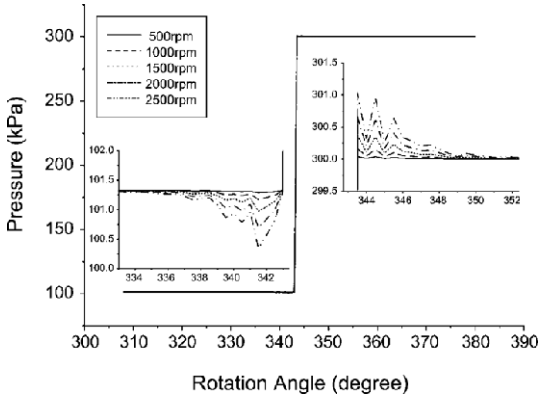

Fig. 15 Pressure pulsation with respect to the rotation velocity of the outer rotor

the suction and delivery groove widths of 4.5 [mm], and the port reference position of the suction port in 343 [degree]. Although the pressure pulsations are increased with the rotation velocity, the maximum pressure overshoot or undershoot in the rotation velocity range of 500～2500 [rpm] are approximately 1 [kPa] which are of the extent negligible in a variety of hydraulic systems. This can be expected from the fact that the effect of the $dV_j/d\alpha$ on the pressure pulsation is remarkably decreased in which $dV_j/d\alpha$ is close to zero, even though the roatation velocity is included in the effective orifice term of Eq. (4). Therefore, we can conclude that although the pressure pulsation is increased with the rotation velocity, its effect can be sufficiently decreased by installing the groove in which the chamber volume rate is close to zero.

6. Conclusions

In gerotor pumps, the pressure drop occurring in the instant that the chamber goes out of the suction port and the pressure rise occurring in the instant that the chamber comes in the delivery port cause the cavitation in the hydraulic system as well as undesired vibration and noise of the mechanical components. In order to cope with these undesired situations, the port plate with the relief grooves was designed in this paper. Then, the effects of the geometric variables, including the groove width and the port reference position,

and the operating conditions, including the delivery pressure and the rotation velocity, on the pressure pulsation of the gerotor pump were investigated through a series of the theoretical analyses. The results obtained in this paper are summarized as follows :

(1) The pressure pulsation can be significantly decreased when the outlet of the suction port and the inlet of the delivery one are positioned at the pointed ends of the chamber where its volume is to be maximized, respectively.

(2) The pressure pulsation can be decreased when the groove width is increased as much as possible so that the opening areas between the chamber and the ports are extended.

(3) The delivery pressure as one of the operating condition of the gerotor pump has no an effect on the pressure pulsation, which is because it is independent of the effective orifice term representing the pressure pulsation.

(4) The pressure pulsation is increased with the rotation velocity given as the other operating condition. However, its effect can be sufficiently decreased by installing the groove in which the chamber volume rate is close to zero.

On the other hand, it is noted that the depth of the groove is specified equally to the height of the gerotor so that the effect of the fluid inertia on the pressure pulsation is not considered in this paper. The groove depth varying according to its length is conceivable to make pressure variations in the gerotor pump more stable. In near future, the effect of the various shapes of the groove on the pressure pulsation in the gerotor pump will be analyzed through theoretical and experimental approaches.

References

Beard, J. E., Pennock, G. R. and Stanisic, M. M., 1989, "The Effects of the Design Parameters on the Generated Curvature and Displacement of Epitrochoidal Gerotor Pumps," *Transactions on Society of Automotive Engineers*, No. 891831.

Beard, J. E., 1992, "The Effects of the Generating Pin Size and Placement on the Curvature and Displacement of Epitrochoidal Gerotors," *Mechanism and Machine Theory*, Vol. 27, No. 4, pp. 373～389.

Colbourne, J. R., 1974, "The Geometry of Trochoid Envelopes and Their Application in Rotary Pumps," *Mechanism and Machine Theory*, Vol. 9, pp. 421～435.

Demenego, A., Vecchiato, D., Litvin, F. L., Nervegan, N. and Mancó, S., 2002, "Design and Simulation of Meshing of a Cycloidal Pump," *Mechanism and Machine Theory*, Vol. 37, No. 3, pp. 311～332.

Gamez-Montero, P. J. and Codina Maciá, E., 2000, "Fluid Dynamic Behaviour of an Internal Rotary Pump Generated by Trochoidal Profiles," *Proceeding of 1st FPNI-PhD Symposium*, Hamburg, pp. 33～47.

Harris, R. M., Edge, K. A. and Tilley, D. G., 1994, "The Suction Dynamics of Positive Displacement Axial Piston Pumps," *ASME, Journal of Dynamic Systems, Measurement, and Control*, Vol. 116, pp.281～287.

Harrison, A. M. and Edge, K. A., 2000, "Reduction of Axial Piston Pump Pressure Ripple," *Journal of Systems and Control Engineering (Part I)*, Vol. 214, No. 1, pp. 53～63.

Kim, D.-I., Ahn, H.-S. and Choi, D.-H., 2000, "Stress Analysis of Epitrochoidal Gerotor for Hydraulic Motor," *Transactions of the Korean Society of Mechanical Engineering (Part A)*, Vol. 24, No. 4, pp. 963～971.

Kim, K.-D., Cho, M.-R., Han, D.-C., Choi, S.-H. and Jang, J.-S., 1998, "An Analytical Study on the Pressure Ripples in a Positive Displacement Vane Pump," *Transactions of the Korean Society of Mechanical Engineering (Part A)*, Vol. 22, No. 11, pp. 1964～1998.

Kim, K. D., Cho, M. R., Han, D. C., Choi, S. J. and Moon, H. J., 1998, "A Study on the Role of Notch and Radius Reduction Ratio in the Balanced Type Vane Pump," *Journal of the Korean Society of Precision Engineering*, Vol. 15, No. 1, pp. 87～93.

Litvin, F. L. and Feng, P.-H., 1996, "Computerized Design and Generation of Cycloidal Gearings," *Mechanism and Machine Theory*, Vol. 31, No. 7, pp.891～911.

Mancó, S., Nervegna, N., Rundo, M., Armenio, G., Pachetti, C. and Trichilo, R., 1998, "Gerotor Lubrication Oil Pump for IC Engines," *Transactions on Society of Automotive Engineers*, No. 982689.

Manfred, C. and Adam, L., 2001, "Distribution of Loads in Cycloidal Planetary Gear (CYCLO) Including Modification of Equidistant," *16th European Mechanical Dynamics User Conference*, Berchtesgaden, pp. 1～11.

Manring, N. D., 2000, "The Dischanrge Flow Ripple of an Axial-Piston Swash-Plate Type Hydrostatic Pump," *Journal of Dynamic Systems, Measurement and Control*, Vol. 122, No. 2, pp. 263～268.

Marnring, N. D., 2003, "Valve-Plate Design for an Axial Piston Pump Operating at Low Displacement," *ASME, Journal of Mechanical Design*, Vol. 125, pp. 200～205.

Mimmi, G. and Pennacchi, P., 1997, "Internal Lobe Pump Design," *Transactions of the CSME*, Vol. 21, No. 2, pp. 109～121.

Saegusa, Y., Urashima, K., Sugimoto, M., Onoda, M. and Koiso T., 1984, "Development of Oil-Pump Rotors with a Trochoidal Tooth Shape," *Transactions on Society of Automotive Engineers*, No. 840454.